Available online at www.sciencedirect.com
ScienceDirect
Trans. Nonferrous Met. Soc. China 23(2013) 1863−1874
Transactions of Nonferrous Metals Society of China
www.tnmsc.cn

Effect of Si-addition as a grain refiner on microstructure and properties of Ti−6Al−4V Alloy

Khaled M. IBRAHIM[1], Abdel Hamied HUSSEIN[2], Mohamed ABDELKAWY[1]

1. Central Metallurgical R&D Institute, CMRDI, Cairo, Egypt;
2. Cairo University, Giza, Egypt

Received 4 February 2013; accepted 26 March 2013

Abstract: Two different Ti alloys were cast in a graphite mould using vacuum induction skull melting furnace. The first alloy was Ti−6Al−4V and the second was Ti−6Al−4V−0.5Si. Silicon as a grain refiner was added into Ti−6Al−4V alloy, and the effects of Si-addition on the microstructure and properties of the as-cast and swaged alloys were investigated. Hot swaging at 900 °C was performed on the cast samples and then two different thermal treatments were applied. The first treatment was done by heating the swaged samples at 1050 °C to produce fine lamella structure, while the second treatment was carried out at 1050 °C and then decreased the temperature to 800 °C for getting coarse lamella structure. An addition of 0.5% Si to Ti−6Al−4V alloy decreased the grain size of the as-cast sample from 627 to 337 μm. There was an increase in ultimate tensile strength of about 25 MPa for the as-cast Ti−6Al−4V−0.5Si alloy compared to Ti−6Al−4V due to the refinement effect caused by Si addition. A maximum ultimate tensile strength of 1380 MPa and a minimum corrosion rate (1.35×10^{-6} mm/a in Hank's solution and 5.78×10^{-4} mm/a in NaCl solution) were reported for the heat treated fine lamella structure of Ti−6Al−4V−0.5Si alloy. The wear rate was decreased to about 50% by adding 0.5% Si at low sliding speeds and to about 73% at high sliding speeds.
Key words: Ti−6Al−4V alloy; silicon; casting; grain refinement; heat treatment; wear

1 Introduction

Titanium has emerged as a very attractive metal for numerous applications. Ti−6Al−4V (Ti-64) is one of the most commonly used titanium alloys in the aviation industry and civil applications due to its high specific strength, high operating temperature and corrosion resistance. The excellent corrosion resistance of Ti-64 is due to the surface oxide film that protects it from corrosive agents such as seawater. Ti-64 is an important $\alpha+\beta$ titanium alloy with an interesting and challenging correlation between mechanical properties and its complex microstructure [1−4]. Titanium alloys normally have a coarse microstructure in the as-cast condition. This coarse microstructure could be attributed to different facts such as cooling rate, solidification, casting procedures and impurities. This condition affects mechanical properties, like strength, ductility and damage tolerance. Therefore, several thermo-mechanical processes are needed to obtain a good balance between static and dynamic properties, which in turn increases time and cost to obtain high quality billets. For other metals and alloys, it is well documented that inoculation using solute elements could refine the grains. A similar approach was used in titanium but there has not been extensive work carried out. BERMINGHAM et al [5] observed that small addition of silicon (<0.6%, mass fraction) produced a significant grain refinement in Ti-64 alloy, which later was observed by other researchers.

Refinement of prior β-grain in cast titanium alloys is believed to improve a number of properties including strength, ductility and fatigue resistance. Despite the associated benefits of controlling prior β-grain size in cast titanium alloys, relatively little research has been conducted into grain refinement of titanium alloys, and no commercial grain refiners currently exist. Some earlier work has reported the grain refinement with various elemental additions, such as B and Br [6,7].

In the present work, two different Ti-alloys were cast in a graphite mould using vacuum induction skull melting (ISM) furnace. The first one was Ti-64 and the

Corresponding author: Khaled M. IBRAHIM; Tel: +96-6558526682, Fax: +20-225010639; E-mail: khaledabouelela@yahoo.com
DOI: 10.1016/S1003-6326(13)62671-0

second was Ti-64−0.5Si, where silicon was added to clarify its role as a solute element in Ti-64. Hot swaging accompanied with thermal treatment process was applied for studying microstructural characteristics and mechanical properties as well as corrosion behavior under all conditions (as-cast, hot swaged and heat treated) for both investigated Ti-alloys (Ti-64 and Ti-64−0.5Si).

2 Experimental

Pure graphite mould was used for casting cylindrical titanium samples with dimensions of 30 mm in diameter and 300 mm in length each. Casting design was made before machining the graphite mould for getting four sound bars. Before melting the titanium alloys, the graphite mould was preheated in a heating chamber inside the ISM furnace to about 900 °C. Hereafter, 10 kg raw material of Ti-64 was heated to reach 1700 °C to melt it under vacuum that reached to 4 Pa. As soon as the charge was melted, a flow of argon was released into the chamber in order to prevent any possible chemical reaction with crucible. Then the molten metal was poured into the graphite mold after holding for 2 min in the crucible. For the second alloy of Ti-64 containing 0.5% Si, the amount of silicon was firstly weighed and ground to <45 μm and then inserted at the bottom of the sprue of the graphite mould. The molten metal was poured into the graphite mould to distribute this amount of silicon homogenously into the four cast Ti-bars. The chemical composition of both investigated Ti-alloys is given in Table 1. To remove the residual stress existing on the surface of the cast bars due to casting, 2.5 mm was removed by turning. The final dimensions of the cast rods became 25 mm in diameter and 250 mm in length which was suitable for the hot swaging process. Swaging was achieved at 900 °C to reduce the cast bars diameter from 25 mm to 8.5 mm in 11 steps. After that two kinds of thermal treatment processes were applied to the swaged samples (Fig. 1). The first treatment was done at 1050 °C for getting fine lamella structure and the second process was applied using step thermal cycle at 1050 °C and then quenching from 800 °C for getting coarse lamella structure. Finally, aging was carried out at 500 °C for 24 h for both samples.

Table 1 Nominal chemical composition of experimental castings

Alloy	Chemical composition/%						
	Al	V	C	O	F	Si	Ti
Ti-64	6.37	4.12	0.02	0.25	0.24	0.02	Bal.
Ti-64−0.5Si	6.26	4.10	0.02	0.25	0.24	0.53	Bal.

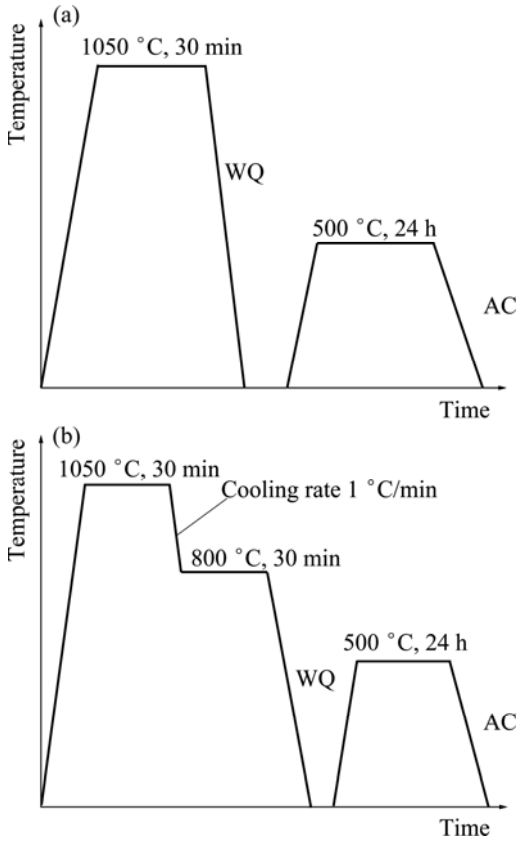

Fig. 1 Heat treatment cycles for getting fine lamella (FL) structure (a) and coarse lamella (CL) structure (b)

Cast and deformed samples were cut out from the rods and polished using conventional techniques. Grain size was also estimated after etching (3 mL of HF, 30 mL of HNO_3, and 67 mL of H_2O). Specimens were photo micrographed using light microscope and scanning electron microscope (SEM). Micro-analysis was carried out using X-ray diffraction (XRD), PC based image analyzer and energy-dispersive spectrometer (EDS). In order to determine the beta transus of each alloy, the solidification path of both Ti-alloys was monitored using heat-flux differential scanning calorimetry (DSC). Mechanical properties including hardness and tensile properties of the different investigated conditions were carried out according to ASTM standards. Further, wear testing was carried out on a pin-on-ring wear testing machine. The wear samples had a rectangular shape of 8 mm×12 mm×12 mm. The test was performed against a stainless steel ring with surface hardness of HRC 63, which was rotated at variable speeds of 270, 330, 400, 465 and 530 r/min and a constant applied load of 90 N for 1 h. After wear testing, the samples were weighed using 0.1 mg precision digital scale to determine the average mass loss of two samples for each condition. The wear rate was then calculated by dividing the mass loss by the testing time. The worn surface of some selected samples was examined using SEM to determine

the wear mechanisms. Corrosion rate was also estimated by using linear polarization resistance (LPR) in two different media. The first one was NaCl solution (3.5%) and the second was Hank's solution.

3 Results and discussion

3.1 DSC results

In this study, DSC was used to determine the beta transus of both Ti-64 and Ti-64−0.5Si alloys, as shown in heating curves in Figs. 2(a) and (b). It is obvious that Ti-64 alloys exhibited higher beta transus than Ti-64−0.5Si. Ti-64 represents a beta transus temperature of 1007 °C, while Ti-64−0.5Si obtains a beta transus temperature of 965 °C. This shift in beta transus temperature is related to the primary effect of Si-addition, where Si is considered β eutectoid forming element. This indicates that Si will stabilize the beta structure due to its solubility in the β phase.

3.2 Microstructure investigation

3.2.1 Ti−6Al−4V alloy

The microstructures of as-cast, swaged (SW) and heat treated Ti-64 samples are shown in Fig. 3. The

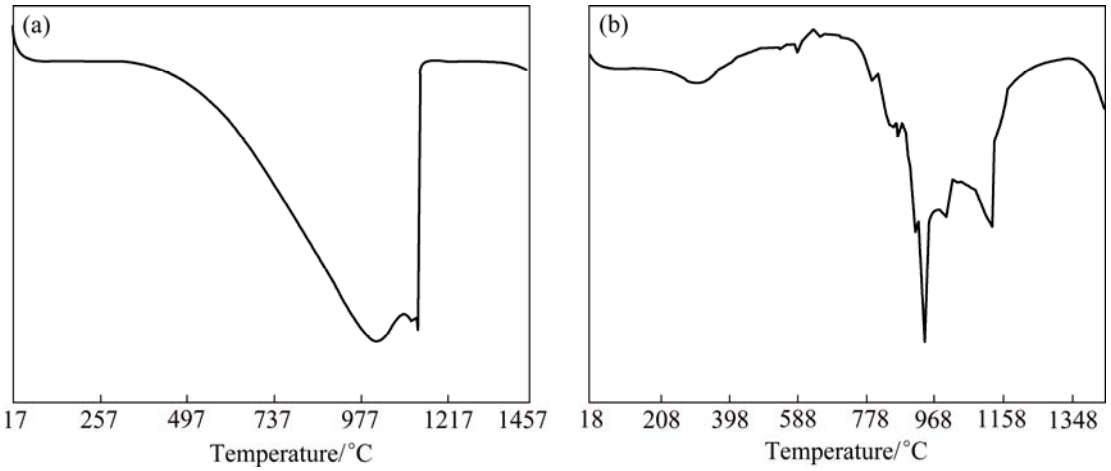

Fig. 2 DCS curves of cast Ti-alloys: (a) Ti-64; (b) Ti-64−0.5Si

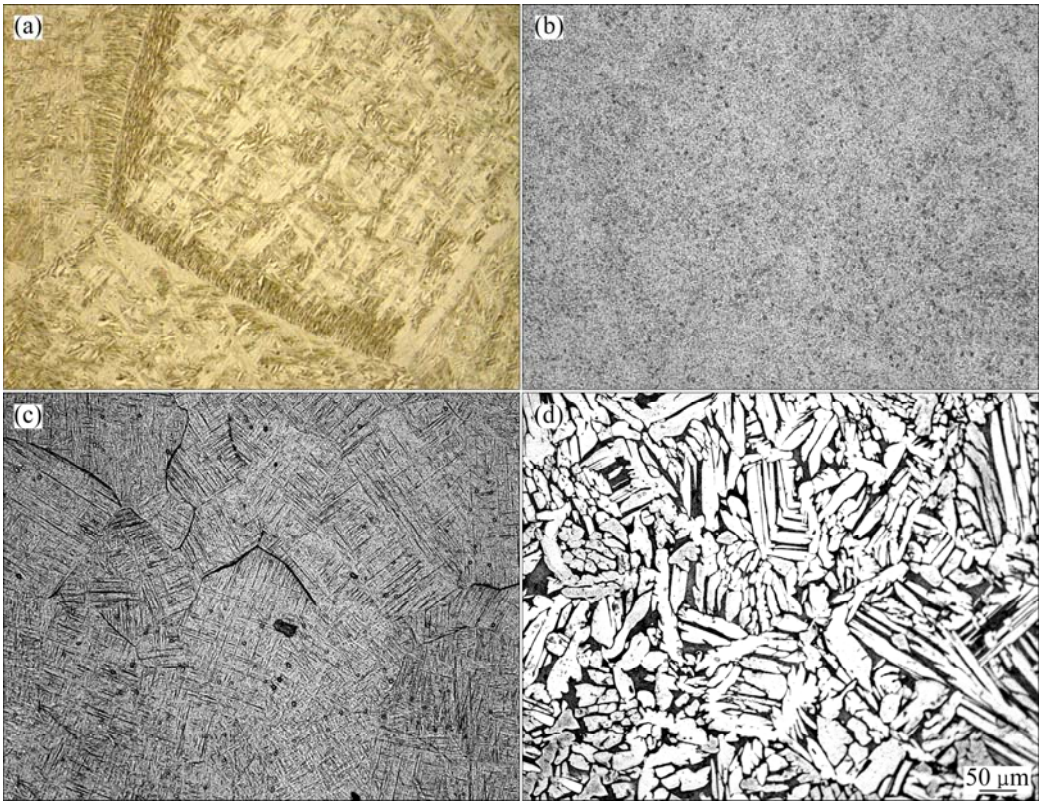

Fig. 3 Microstructures of Ti-64 at different conditions: (a) As-cast; (b) Swaged; (c) Fine lamellar; (d) Coarse lamellar

as-cast sample shows $\alpha-\beta$ colony structure with alternate layers of hexagonal closed packed (HCP) α and thin body-centered cubic (BCC) β distributed in prior β grains, (Fig. 3(a)). The plate-type $\alpha-\beta$ lathes orient along preferred orientations (per Burger's orientation relationships between α and β) to form colonies [3,4]. Several of these colonies are randomly oriented weave structure. The size of the prior β-grains is in the range of 0.9−2 mm while the colonies range in the size from 580 to 630 μm.

The swaged samples show a structure consisting of fine equiaxed $\alpha+\beta$ because these samples were hot swaged at 900 °C (i.e., at $\alpha+\beta$ temperature range) (Fig. 3(b)). It is obvious that the as-cast lamellar structure is broken down into equiaxed fine structure by swaging which is normally achieved by extensive plastic deformation well below the β-transus. The swaged condition shows very fine grains of about 80 μm. This finding is in agreement with the study done by TAMIRISAKANDALA et al [7]. The mechanism of forming such structure by hot swaging involves shearing of lamellae during deformation and subsequent rounding by diffusion process, which is driven by urge to minimizing the surface area for attaining thermodynamically the lowest energy state [8,9]. The heat-treated samples show another feature of microstructure, as shown in Figs. 3(c) and (d). Generally, the heat-treated samples show lamellae structure, but these lamellae are different in size and distribution depending on the quenching temperature and cooling rate. Depending on the cooling rate, the lamellae could be fine or coarse. Rapid quenching from above β-transus leads to a martensitic structure, very fine needle-like microstructure, and results also in forming fine β-phase. In this study, Ti-64 samples were subjected to different solution treatments. Figure 3(c) shows fine lamellar β structure and some amounts of α' martensitic structure because these samples were rapidly quenched from 1050 °C in which this temperature (1050 °C) is considered to be above β-transus for the investigated Ti-64 alloy. While, the other samples that were rapidly quenched from 800 °C obtained a coarse lamella structure of α and β (Fig. 3(d)).

3.2.2 Ti−6Al−4V−0.5Si alloy

The effect of Si-addition on the microstructure of Ti-64−0.5Si was also investigated. The binary Ti−Si phase diagram, shown in Fig. 4, provides a reasonable guide to understand the solidification sequence and microstructural development of Ti-64−0.5Si alloy. Growth restriction theory suggests that silicon is considered a refiner to the prior β grain by contributing and development of the constitutionally undercooled zone. Silicon is directly responsible for refining the as-cast grain size through the nucleant mechanism and precipitating few amounts of intermetallic silicides that were observed in the as-cast structure. Further, consultation of the binary Ti−Si phase diagram suggests that no intermetallics are present in the liquid before β-Ti solidification. Despite this, the possibility still exists that nuclei can indirectly be introduced by adding small amount of silicon, i.e., introduction of impurity nuclei within the silicon addition [10−13]. These intermetallic silicides play of course an important role in refining the as-cast structure of Ti-64 alloy containing Si.

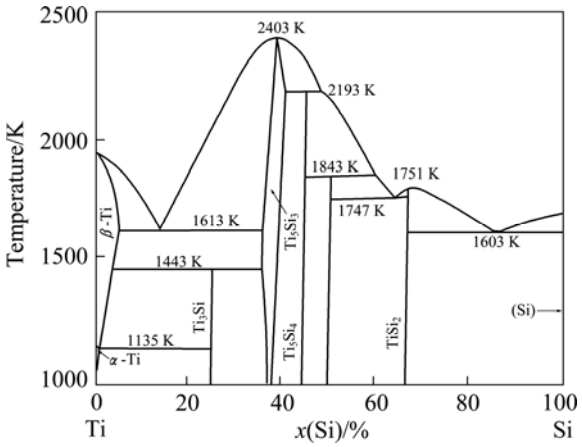

Fig. 4 Binary Ti−Si phase diagram

The as-cast structure of Ti-64−0.5Si consists of α and β phases (Fig. 5(a)). This structure obtains a grain size in the range of 310−350 μm. It could be said that an addition of 0.5% Si to the molten metal of Ti-64 can reduce the grains size to the half, which will directly have a great influence on the mechanical properties. The swaged Ti-64−0.5Si samples show also a microstructure similar to Ti-64 alloy, but it seems finer than the last one (Fig. 5(b)). This is because the structure before deformation has a fine structure, consequently the deformed structure will be much finer compared to Ti-64 alloy, especially the degree of deformation is the same in both cases. The estimated grain size of the swaged Ti-64−0.5Si is in the range of 30−32 μm (Fig. 6). Figures 5(c) and (d) show the microstructures of the heat treated samples with an addition of 0.5% Si. The samples show a structure similar to the previous one, Ti-64, in which quenching from 1050 ºC obtained fine lamellar structure (martensitic structure), but the difference lies in the fineness of the grain size. As shown in Fig. 5(c), complete grains can be seen in the microstructure compared to Ti-64 alloy (Fig. 3(c)). In addition, quenching from 800 ºC reveals a coarse lamellar structure similar to Ti-64, as shown in Fig. 5(d). It is often observed in grain refinement studies that the point of saturation is usually reached with increasing the grain refiner additions to a certain limit and then no further refinement can be achieved. BERMINGHAM et al [5]

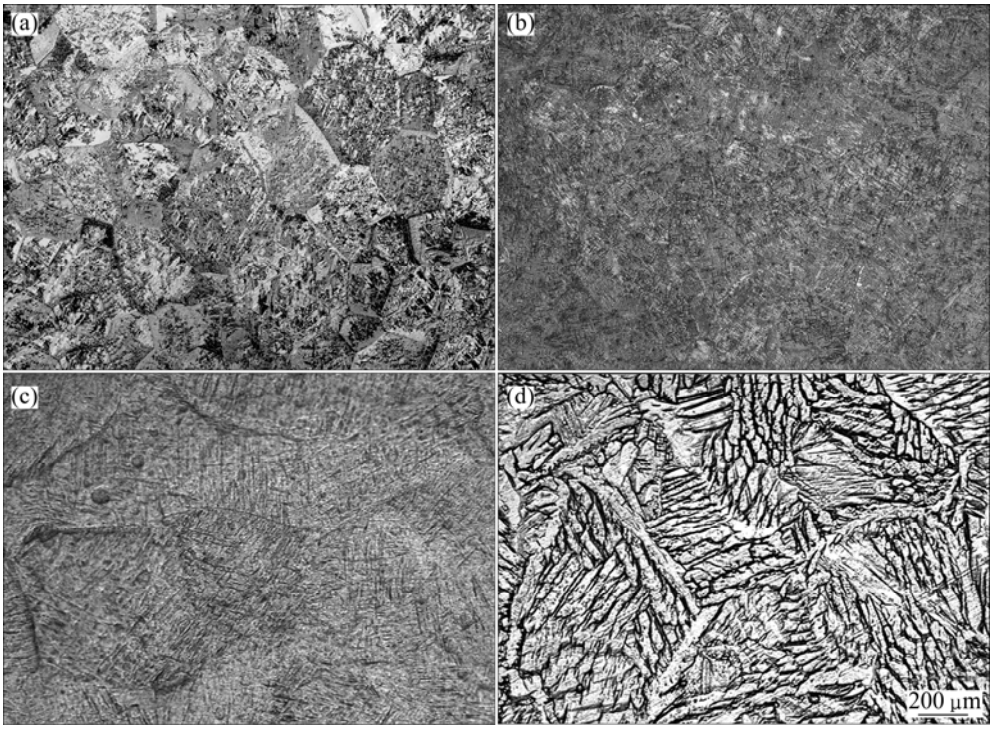

Fig. 5 Microstructures of Ti-64−0.5Si at different conditions: (a) As-cast; (b) Swaged; (c) Heat treated fine lamellar; (d) Heat treated coarse lamellar

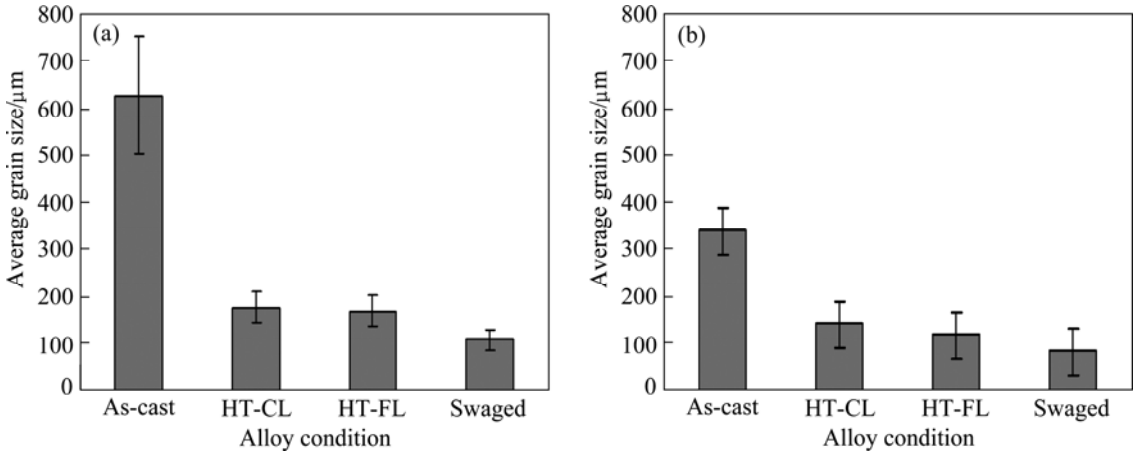

Fig. 6 Average grain size of Ti-64 (a) and Ti-64−0.5Si (b)

found that the saturation point appears to occur when silicon content exceeds 0.6% (mass fraction), but ZHU et al [6] found that a similar saturation point that cannot be reached until much higher amount of silicon can be added (~1.75%Si).

The degree of grain refinement relies on the balance between latent heat production and heat extraction at the solid/liquid interface. The rate of latent heat production is limited by solute partitioning at solid/liquid interface and diffusion in the melt. The idealized binary systems of Maxwell−Hellawell model mentioned in Refs. [5,9,10] proposed that diffusion limited growth rate of a sphere at a given melt undercooling and sphere radius is inversely proportional to thermodynamic quantity, as stated in equation: $Q=m_l(k-1)C_0$, where Q is the growth restriction factor, m_l the slope of liquidus, K the solute partition, $K=C_S/C_L$ (C_S and C_L are solute contents of the solid and liquid equilibrium at the interface between them and C_0 is solute content). The basis of the Maxwell–Hellawell model is restricted to the growth of already nucleated grains permitted continuing nucleation in the undercooled melt until the total latent heat release is sufficient to cause recalescence and loss of undercooling. The growth restriction factor "Q" is a good parameter to describe the solute effects on grain refinement, where Q for silicon is $18.7C_0$ [5]. Based on the aforementioned

Maxwell−Hellawell model, the grain refinement mechanism of Ti-64−0.5Si can be discussed. It is well known that the grain size obtained after solidification is determined by competition between the nucleation and growth rates. The appearance of equiaxed grains in the as-cast condition implies that super cooling arising from the change in composition (constitutional) is more important during solidification than thermal under-cooling. Once a nucleus is formed, its growth is influenced by kinetics of atom attachment to interface, capillarity and diffusion of heat and mass at the interface and away from the interface [14−17]. Silicon rejected at solid/liquid interface is likely to influence these factors and restrict the growth of existing nuclei [5]. The XRD study has been carried out on the Ti-64−0.5Si samples and shows a small amount of intermetallic compound (Fig. 7). According to the binary Ti−Si phase diagram, this intermetallic compound is Ti_3Si that contains Si in the range of 35.5% to 39.5% (mole fraction).

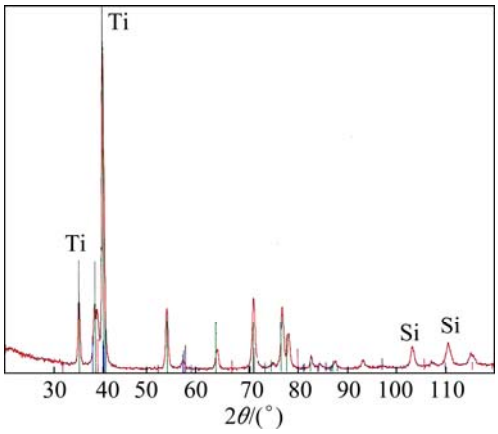

Fig. 7 XRD pattern of Ti-64−0.5Si alloy

3.3 Mechanical properties

3.3.1 Hardness

The hardness results of the as-cast, swaged and heat treated alloys are shown in Fig. 8. Solution treatment and subsequent aging at 500 °C for 24 h led to an increase in hardness compared to the as-cast condition. Generally, Ti-64−0.5Si obtained higher hardness compared Ti-64 in the as-cast, swaged and heat treated conditions. Minimum hardness was obtained in the as-cast condition due to the coarse grain structure compared the swaged and heat treated ones. On the other hand, the maximum hardness (HV 450) was obtained for the heat treated Ti-64−0.5Si alloy with fine lamellar structure. Moreover, the heat treated Ti-64 alloy with fine lamellar structure revealed a hardness value of HV 440, in which Si-addition has no large influence. This finding is in agreement with SEN et al [17], where they found that there was a small enhancement in mechanical properties by adding 0.1% B. Therefore, it could be concluded that the microstructure feature plays a big role in determining the hardness values of the investigated Ti-alloys. For example, the heat treated coarse lamellar structure showed lower hardness compared to the fine lamellar structure. The heat treated Ti-64 and Ti-64−0.5Si with coarse lamellar structure showed hardness values of HV 350 and HV 375, respectively. Thereby, refining of the $\alpha+\beta$ structure by adding 0.5% Si achieved an increase in hardness of about 7% for the studied Ti-alloys. Similarly, the swaged samples obtained higher hardness compared to the as-cast samples due to the refining effect caused by applying severe plastic deformation on the cast structure, where the grain size of T-64 alloy decreased from 630 μm for the cast condition to 80 μm in the swaged Ti-64 alloy. In addition, existing of some intermetallic silicides in Ti-64−0.5Si samples has also a role in increasing the hardness value comparing to the conventional Ti-64 samples.

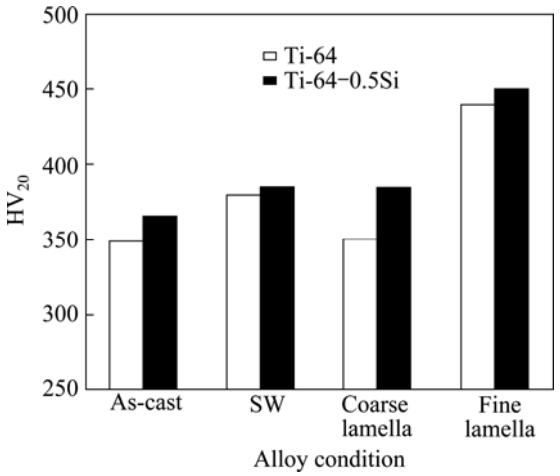

Fig. 8 Hardness values of Ti-64 and Ti-64−0.5Si alloys at different conditions

3.3.2 Tensile properties

Tensile properties of both investigated Ti alloys were determined. It was found that they were typically dependent on the microstructure features. Figure 9 shows the tensile properties of the examined Ti alloys. The as-cast Ti-64 showed UTS of 1050 MPa, and by adding 0.5% Si the UTS increased to 1075 MPa. This increase in UTS (about 25 MPa) is due to the refining effect caused by Si-addition. The maximum UTS was reported for the heat treated fine lamellar structure, where Ti-64 obtained UTS of 1300 MPa and Ti-64−0.5Si revealed UTS of approximately 1380 MPa. The minimum UTS was reported for the heat treated coarse lamellar structure, where Ti-64 and Ti-64−0.5Si showed UTS of 1000 and 1070 MPa, respectively. This finding is consistent with that reported by BERMINGHAM et al [11−13] on the effect of Si-addition on mechanical properties of Ti alloys. Figure 9(b) shows the effect of Si-addition and

heat treatment on yield strength of the studied Ti alloys. The yield strength had the same trend as ultimate tensile, where Si-addition improved the yield strength compared to the conventional Ti-64 alloy. It is possible to mention that improvement in yield strength in all conditions, as-cast and swaged conditions, is primarily related to the Hall−Pitch mechanism where the yield strength is inversely correlated with the grain size [15,16]. This indicates that the enhancement in strength with adding Si is primarily due to the microstructural refinement. This finding is in agreement with the study done by SEN et al [17] on Ti-64 with an addition of B as a grain refiner. It is also consistent with the earlier research work showing that the tensile and compressive yield strengths of Ti-64 increased with increasing α plate/lath size due to the reduction in the effective slip length [18]. The Hall−Pitch mechanism is more pronounced in the swaged condition, where Ti-64−0.5Si obtained higher yield strength than Ti-64. This is because both alloys were subjected to the same degree of severe plastic deformation (swaging process). But, Ti-64−0.5Si started with much finer structure, due to Si-addition, compared to the Ti-64 alloy.

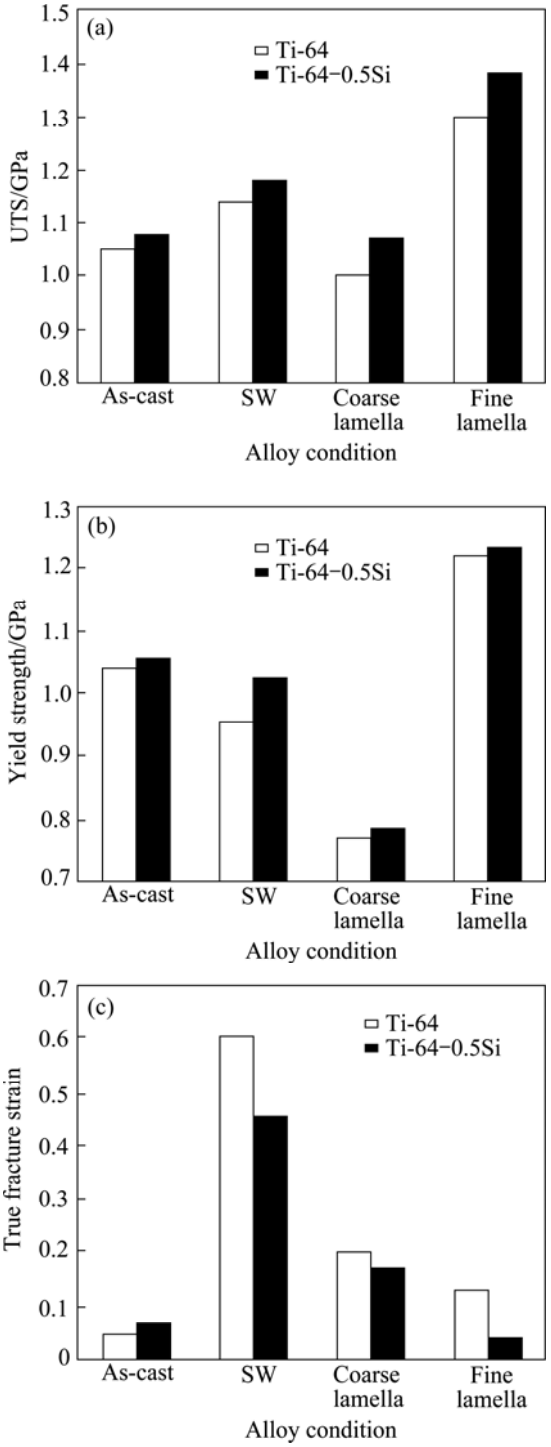

Fig. 9 Tensile properties of Ti-alloys: (a) UTS; (b) YS; (c) ε_f

The minimum true fracture strain (ε_f) was also obtained for the as-cast conditions due to their coarse grains as well as the structure heterogeneity (Fig. 9(c)). As-cast Ti-64 showed ε_f of 0.043%, while Ti-64−0.5Si revealed relatively higher ε_f of about 0.068% due to the refining caused by Si-addition. The maximum ε_f was obtained for the swaged condition because the swaged samples had the finest globular $\alpha+\beta$ structure which is characterized by high ductility [19]. However, the heat treated samples with fine lamellar structure obtained lower values of ε_f due to their high strength values and existence of α' martensitic structure. Of course, coarse lamellar structure obtained higher ε_f compared to fine lamellar one because the coarse lamellar structure had lower strength and hardness compared to the fine one due to existence of higher amount of α-phase in the structure.

The fracture surface of some selected tensile samples was examined using SEM. It was noticed that the fracture appearance of both studied Ti-alloys (Ti-64 and Ti-64−0.5Si) was approximately similar. Therefore, this study was based only on Ti-64−0.5Si alloy. Figure 10 illustrates the fracture surfaces of the heat treated and swaged Ti-64−0.5Si samples. The fracture surface of fine lamellar structure (Fig. 10(a)) showed a quasi-cleavage fracture due to the presence of fine $\alpha+\beta$ phase and some of α' martensitic structure. Because the fine lamellar structure obtained low ductility, the fracture surface showed also large area of cleavage fracture which was denoted to α phase. The dimple fracture was related to the β phase. Because the maximum ductility was obtained for the swaged alloy, the fracture surface revealed high number of dimples, as shown in Fig. 10(b). It was also noticed that the coarse lamellar structure (Fig. 10(c)) showed relatively similar fracture surface mode for the swaged samples, but some cracks were found at the grain boundaries. The fracture features or appearance of the coarse lamellar structure seemed bigger than the swaged one due to the coarsening happened by quenching from 800 °C. It is also known that the primary α (α_p) can influence the ductility of $\alpha-\beta$ Ti alloys by changing the shape and size of the primary α.

Coarsening of α_p as well as the change from globular to acicular of the α_p led to a reduction in ductility. The reason for both observations was the increased "effective" size or slip length of the soft α_p favoring early crack nucleation. Moreover, the presence of grain boundary α lowered ductility since the strain localized in the soft β-film led to crack nucleation and fracture at grain boundaries [18,20].

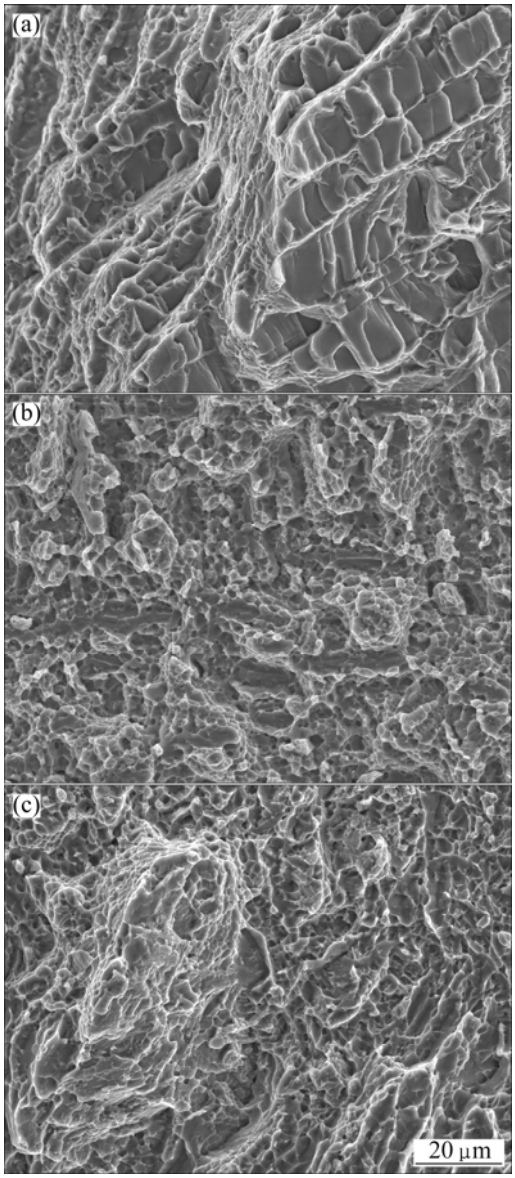

Fig. 10 Fracture surfaces of tensile samples: (a) Fine lamellar; (b) Swaged; (c) Coarse lamellar

3.4 Wear property

In this study, the effect of Si-addition and sliding speed on wear rate of Ti-64 was investigated. Figure 11 represents the wear rate of Ti alloys as a function of sliding speed. The estimated values of wear rates in all conditions indicated that the wear rates increased with increasing the sliding speed. Both alloys (Ti-64 and Ti-64−0.5Si) showed the same behavior with increasing the sliding speed, where the minimum wear rate was reported for the heat treated fine lamellar structure and the maximum one was obtained for the heat treated samples with coarse lamellar structure. According to the Archard's law, the volumetric loss of the material is inversely proportional to hardness value of the material [3]. This implies that the higher the hardness of the material is, the smaller the volume loss is. The investigated Ti-64 alloy exhibited significant difference in hardness, therefore the experimental sliding wear data correlated well with Archard's law [3].

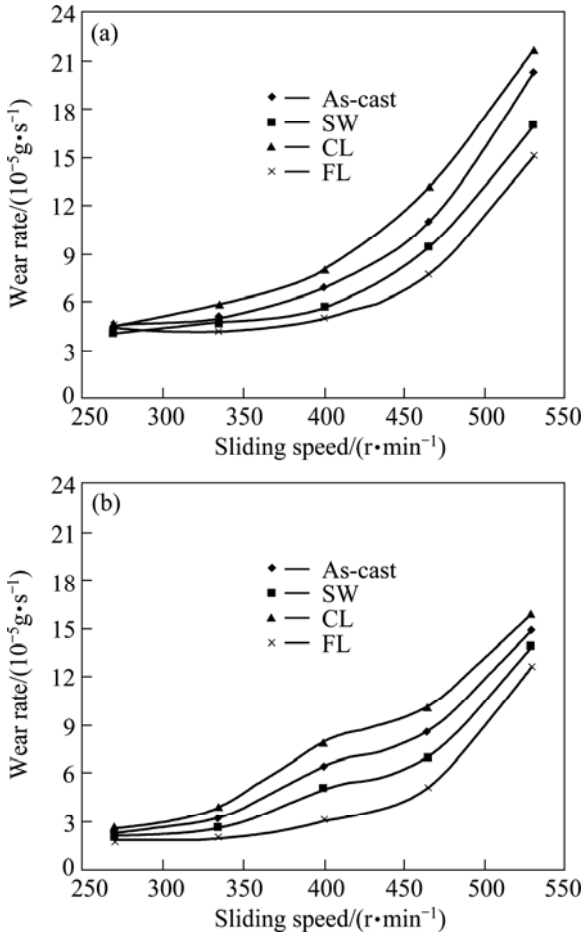

Fig. 11 Wear rate of Ti-64 (a) and Ti-64−0.5Si (b) alloys

The heat treated samples with fine lamellar structure showed the lowest wear rate among all other investigated alloys due to the highest hardness value compared to the others. In addition, the grain refinement due to swaging or heat treatment and increasing in dislocation density decreased significantly the wear rate of the studied Ti alloys. Moreover, existing of α' martensitic structure decreased the wear rate as well. Therefore, the minimum wear rate was reported for the heat treated samples with fine lamellar structure and the maximum value was obtained for the heat treated samples with coarse lamellar structure. It is also noticed that by adding 0.5% Si to Ti-64 alloy, the wear rate significantly

decreased in all conditions. At a low sliding speed, the wear rate decreased to 50% by adding 0.5% Si to Ti-64 alloy due to the formation of hard Ti_3Si particles as well as the refinement effect occurring in the microstructure. But at a higher sliding speed (e.g., 530 r/min), the wear rate of Ti-64−0.5Si alloy was estimated to be approximately 73% compared to Ti-64 alloy. The shear stress over the worn surface at a lower sliding speed was more pronounced, therefore there was a big difference in wear rate by adding Si to Ti-64 alloy. But at high sliding speeds, the shear stress cannot be considered the main factor because high sliding speed causing softening for the worn surface due to the existence of a high amount of friction between the sample and the counterpart (the ring).

In order to gain more insight into the wear mechanism, the worn surfaces of some selected samples were studied using SEM (Figs. 12 and 13). The micrographs show typical worn surface morphologies of the samples tested at low or high sliding speeds. The morphologies of the samples worn at the intermediate sliding speed are not included here because they demonstrated intermediate characteristics between the two extremes. Both alloys showed approximately the same worn surface features at low or high sliding speeds. Figure 12 shows the worn surfaces of Ti-64 alloy

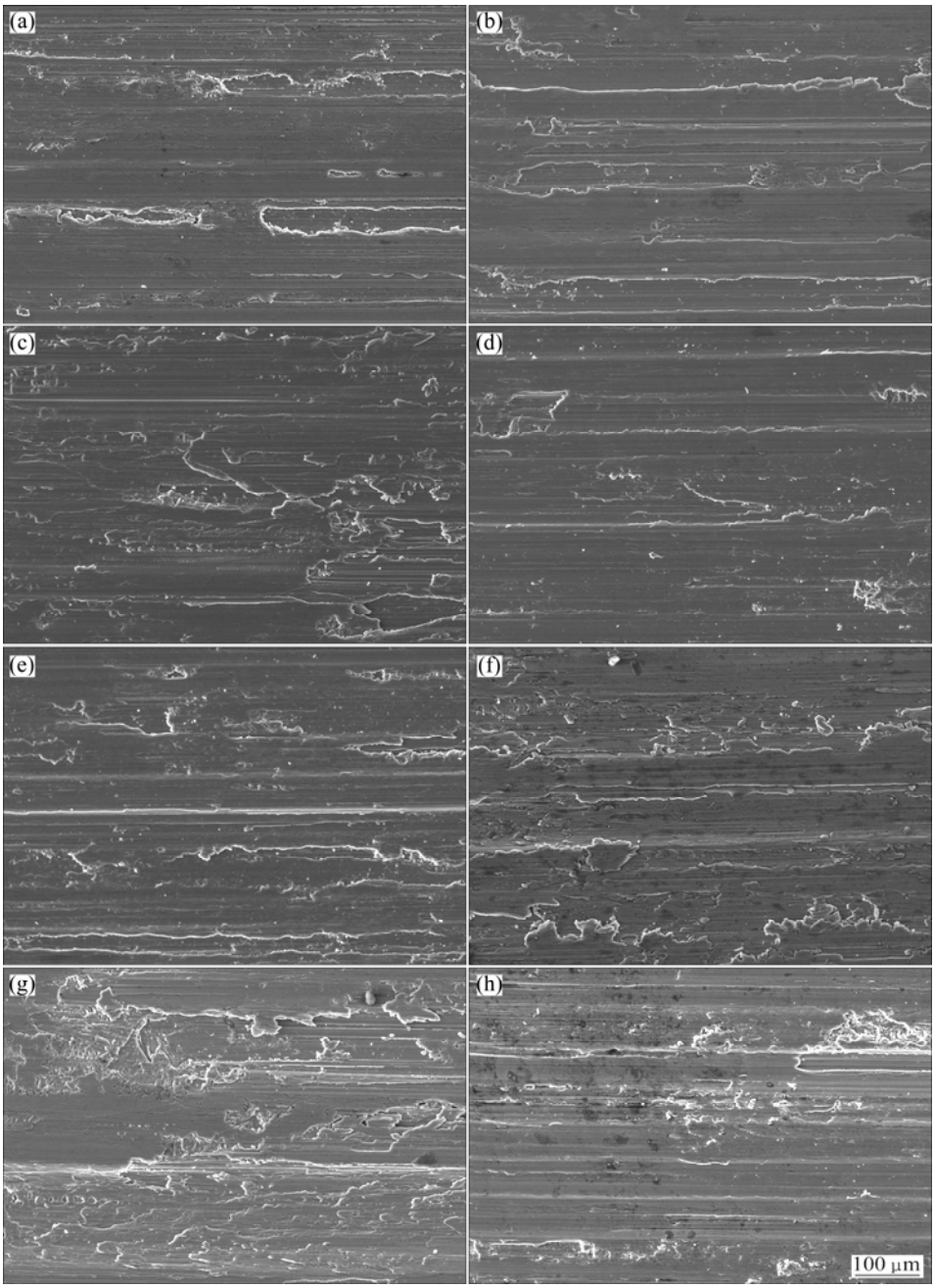

Fig. 12 SEM micrographs showing worn surfaces of Ti-64 alloy: (a) As-cast, 400 r/min; (b) SW, 400 r/min; (c) CL, 400 r/min; (d) FL, 400 r/min; (e) As-cast, 530 r/min; (f) SW, 530 r/min; (g) CL, 530 r/min; (h) FL, 530 r/min

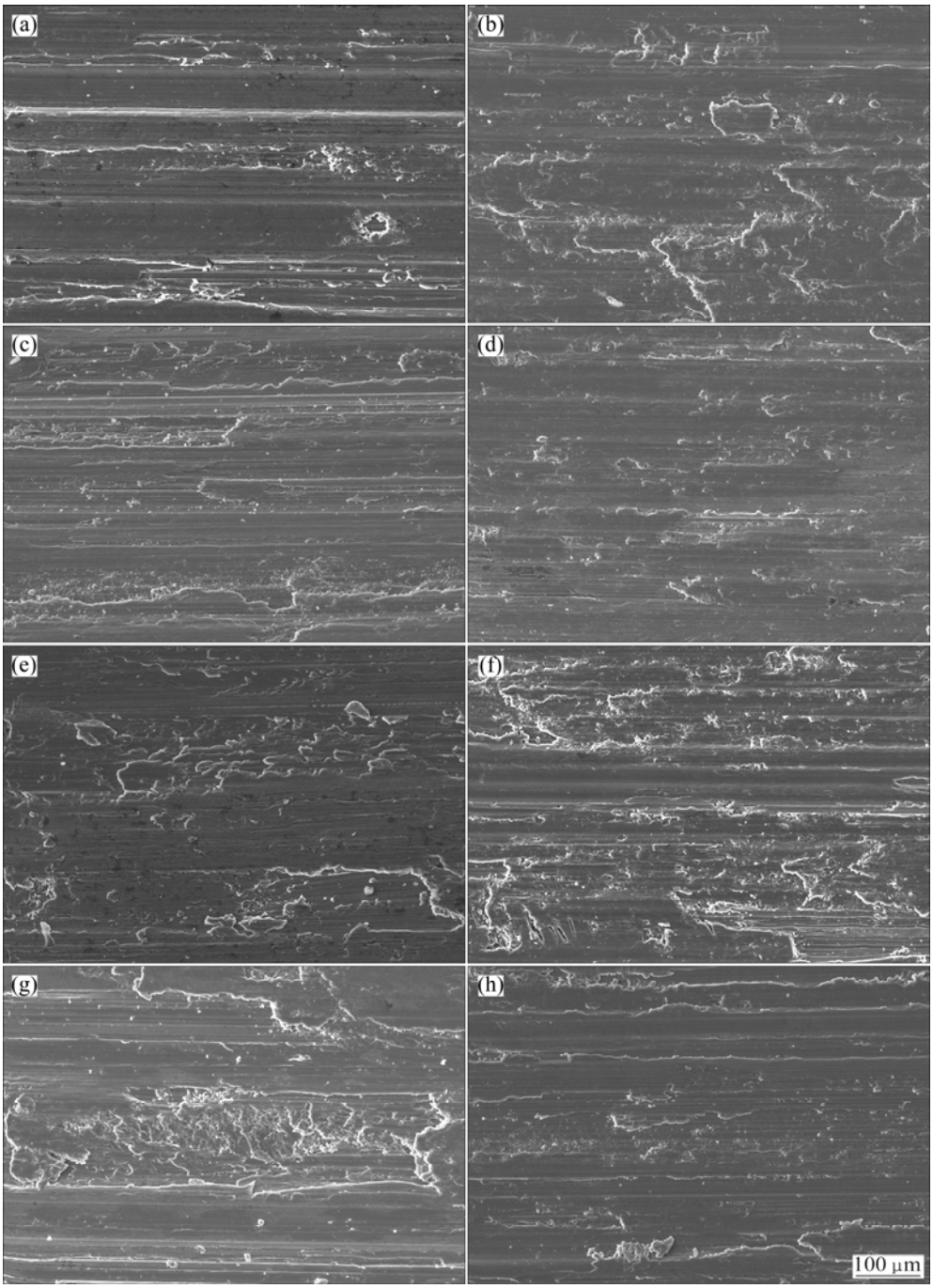

Fig. 13 SEM micrographs of Ti-64−0.5%Si alloy: (a) As-cast, 400 r/min; (b) SW, 400 r/min; (c) CL, 400 r/min; (d) FL, 400 r/min; (e) As-cast, 530 r/min; (f) SW, 530 r/min; (g) CL, 530 r/min; (h) FL, 530 r/min

in all conditions at sliding speeds of 400 and 530 r/min, respectively. Evidences of continuous sliding marks with plastically deformed grooves were seen on the wear tracks independently of the sliding speed. However, the extent of plastic deformation or ploughing was found to be more pronounced in the case of higher sliding speed (530 r/min) (Figs. 12(f)−(h)). Only shallow grooves and scratching can be observed in the case of low sliding speed (400 r/min) (Figs. 12(a)−(d)). In addition, lamination wear mechanism can be observed at low sliding speed and it is found to be clearer for the heat treated samples with coarse lamellar structure because of their low hardness (Fig. 12(c)). While delamination wear mechanism can be found with higher sliding speeds and its features were more visible in the case of low hardness, as shown in Fig. 12(g), for the heat treated samples with coarse lamellar structure. Figure 13 shows the worn surfaces of Ti-64−0.5Si in all conditions at low or high sliding speeds. Low sliding speed obtained lighter scratches over the worn surface in all conditions

compared to Ti-64 due to higher hardness values of Ti-64−0.5Si. In addition, Ti-64−0.5Si showed also lamination wear mechanism at low sliding speed (400 r/min), as seen in Figs. 13(a)−(d). At higher sliding speed (530 r/min), the wear mechanism can be defined as delamination, as shown in Figs. 13(e)−(h). It is also obvious that the plastic deformation or ploughing over the worn surface of Ti-64−0.5Si samples seemed to be lighter than that seen in Ti-64 sample.

3.5 Corrosion behaviour

It was necessary to evaluate the corrosion behavior of the studied Ti alloys in two different media. The first one was NaCl (3.5%) which is important for the engineering industry, such as petroleum industry. The second medium was Hank's solution to evaluate the corrosion performance of Ti-64 as a medical implant material. The correlation between microstructure features, Si-content and heat treatment process was made to get the optimum conditions that satisfy the minimum corrosion rate. The corroding species were assumed to be Ti in the above calculations. The calculated corrosion rates of the investigated Ti alloys (Ti-64 and Ti-64−0.5 Si) are shown in Fig. 14. It is clear that an addition of 0.5% Si enhanced the corrosion resistance, where the corrosion rate of Ti-64−0.5Si was approximately half in magnitude compared to Ti-64 alloy. In addition, the maximum corrosion rate was reported for the as-cast condition in both alloys due to the coarse grain size compared to the other conditions as well as the heterogeneity existing in as-cast structure. By refining the as-cast structure using hot swaging, the corrosion resistance was relatively improved. The most enhancements in corrosion resistance were obtained by applying thermal heat treatment to getting fine lamellar structure which revealed the minimum corrosion rates. These observations were noticed for the samples tested in NaCl and Hank's solutions. Therefore, the corrosion resistance of the studied cast Ti-64 can be improved by adding 0.5% Si and applying thermal treatment at 1050 °C to getting fine lamellar structure.

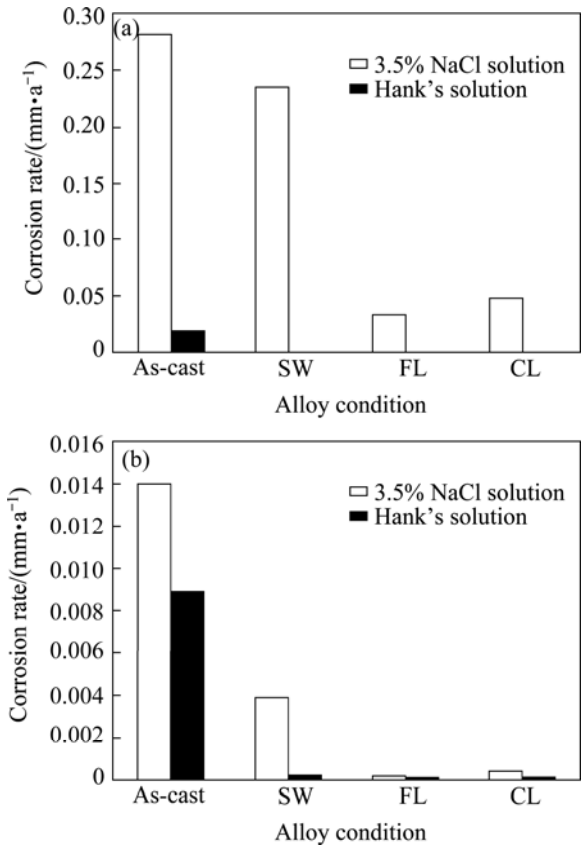

Fig. 14 Corrosion rates of Ti alloys at different conditions and media: (a) Ti-64; (b) Ti-64−0.5Si

4 Conclusions

1) An addition of 0.5% Si to Ti-64 alloy decreased the grain size in the as-cast structure from 627 to 337 μm. Consequently by applying hot swaging at 900 °C, the grain size of the studied samples decreased from 80 to 40 μm.

2) An addition of 0.5% Si to the cast Ti-64 alloy enhanced the mechanical properties by about 10%. Optimum mechanical properties (UTS=1380 MPa, YS=1250 MPa and ε_f=0.14%) and minimum corrosion rates (1.35×10^{-6} mm/a in Hank's solution, and 5.78×10^{-4} mm/a in NaCl solution) were obtained for the heat treated Ti−6Al−4V−0.5Si alloy with fine-lamellar structure.

3) The wear rate decreased to 50% by adding 0.5% Si to Ti-64 alloy at a low sliding speed, and decreased to 73% at a high sliding speed.

4) Lamination wear mechanism was involved at a low sliding speed and delamination wear mechanism was observed at a high sliding speed.

Acknowledgements

The authors would like to thank the Laboratory of Corrosion and Surface Protection at CMRDI, Egypt for carrying out the corrosion tests and also many thanks to Clausthal University of Technology-IWW (Prof. L. WAGNER), Germany for performing the swaging process.

References

[1] TOMOYUKI K. Recent development in the research, production and application of titanium in Japan [C]//Proceeding of the 11th World Conference on Titanium. Japan, 2007.

[2] MATHEW J, DONACHIE J. Introduction to titanium and titanium alloys [M]//Titanium and titanium alloys. Source Book. 1973.

[3] LUTJERING G, WILLIAMS J C. Titanium [M]. Springer, 2003.

[4] LEYENS C, PETERS M. Titanium and titanium alloys:

Fundamentals and applications [M]. Germany: WILEY-VCH, 2003.
[5] BERMINGHAM M J, MACDOLAND S, DARGUSCH M S, StJOHN D H. The mechanism of grain refinement of titanium by silicon [J]. Scripta Materialia, 2008, 58: 1050−1053.
[6] ZHU J, KAMIYA A, YAMADA T, WATAZU A, SHI W, NAGANAMA K. Effect of silicon additions on microstructure and mechanical properties of cast titanium alloys [J]. Materials Transactions, 2001, 42: 336−341.
[7] TAMIRISAKANDALA S, BHAT R B, TILY S J, MIRACLE D B. Grain refinement of cast titanium alloys via trace boron addition [J]. Scripta Materialia, 2005, 53: 1421−1426.
[8] CHRAPONSKI J. The effect of lamellar separation on the properties of a Ti−46Al−2Nb−2Cr intermetallic alloy [J]. Materials Characterization, 2006, 56: 414−420.
[9] MIN X H, EMURA S, SEKIDO S, NISHIMURA T, TSUCHIYA K, TSUZAKI K. Effects of Fe addition on tensile deformation mode and crevice corrosion resistance in Ti−15Mo alloy [J]. Materials Science and Engineering A, 2010, 527: 2693−2701.
[10] BERMINGHAM M J, MACDOLAND S D, DARGUSCH M S, StJOHN D H. Microstructures of cast titanium alloys [J]. Materials Forum, 2007, 31: 84−89.
[11] BERMINGHAM M J, MACDOLAND S D, DARGUSCH M S, StJOHN D H. Grain-refinement mechanisms in titanium alloys [J]. Journal of Materials Research, 2008, 23: 97−104.
[12] BERMINGHAM M J, MACDOLAND S D, NOGITA K, StJOHN D H, DARGUSCH M S. Effects of boron on microstructure in cast titanium alloys [J]. Scripta Materialia, 2008, 59: 538−541.
[13] BERMINGHAM M J, MACDOLAND S D, StJOHN D H, DARGUSCH M S. Segregation and grain refinement in cast titanium alloys [J]. Journal of Materials Research, 2009, 24: 1529−1535.
[14] BOEHLERT C J, COWEN C J, TAMIRISAKANDALA S, MCELDOWNEY D J, MIRACLE D B. In situ scanning electron microscopy observations of tensile deformation in a boron-modified Ti−6Al−4V alloy [J]. Scripta Materialia, 2006, 55: 465−468.
[15] BERMINGHAM M J, MACDOLAND S D, StJOHN D H, DARGUSCH M S. Beryllium as a grain refiner in titanium [J]. Journal of Alloys and Compounds, 2009, 481: 120−123.
[16] BERMINGHAM M J, MACDOLAND S D, DARGUSCH M S, StJOHN D H. Latest developments in understanding the grain refinement of cast titanium [J]. Materials Science Forum, 2009, 618−619: 315−318.
[17] SEN I, TAMIRISAKANDALA S, MIRACLE D B, RAMAMURTY U. Microstructural effects on the mechanical behaviour of B-modified Ti−6Al−4V alloys [J]. Acta Materialia, 2007, 55: 4983−4993.
[18] MIN X H, EMURA S, NISHIMURA T, ZHANG L, TAMILSELVI S, TSUCHIYA K, TSUZAKI K. Effects of α phase precipitation on crevice corrosion and tensile strength in Ti−15Mo alloy [J]. Materials Science and Engineering A, 2010, 527: 1480−1488.
[19] MATSUMOTO H, YONEDA H, SATO K, KUROSA S, MAIRE E, CHIBA A. Room-temperature ductility of Ti−6Al−4V alloy with α' martensite microstructure [J]. Materials Science and Engineering A, 2011, 528: 1512−1520.
[20] IBRAHIM K M, MHAEDE M, WAGNER L J. Microstructure evolution and mechanical properties of heat treated LCB titanium alloy [J]. Transactions of Nonferrous Metals Society of China, 2012, 22: 2609−2615.

添加晶粒细化剂硅对 Ti−6Al−4V 合金组织和性能的影响

Khaled M. IBRAHIM[1], Abdel Hamied HUSSEIN[2], Mohamed ABDELKAWY[1]

1. Central Metallurgical R&D Institute, CMRDI, Cairo, Egypt;
2. Cairo University, Giza, Egypt

摘　要：采用真空感应凝壳熔炼工艺在石墨模中制备 Ti−6Al−4V 和 Ti−6Al−4V−0.5Si 两种钛合金。将硅作为一种晶粒细化剂加入到 Ti−6Al−4V 合金中，考察添加硅对铸态和模锻态 Ti−6Al−4V 合金组织和性能的影响。铸态合金先在 900 °C 下进行热模锻处理，然后分别进行两种不同的热处理。一种是将模锻样品在 1050 °C 下保温 30 min，然后水淬以获得细小的层片状组织；另一种是将模锻件在 1050 °C 下保温 30 min，然后再在 800 °C 下保温 30 min，以获得粗大的层片状组织。Ti−6Al−4V 合金中添加 0.5%Si 后，铸态合金的晶粒尺寸从 627 μm 减小到 337 μm，其极限抗拉强度增加约 25 MPa。具有细小、层片状组织的 Ti−6Al−4V−0.5Si 合金的最大极限抗拉强度为 1380 MPa，在 Hank 溶液和 NaCl 溶液中的腐蚀速度分别为 1.35×10^{-6} 和 5.78×10^{-4} mm/a。Ti−6Al−4V 合金中添加 0.5%Si 后，在低滑动速度下的磨损率降低 50%，在高滑动速度下的磨损率降低约 73%。

关键词：Ti−6Al−4V 合金；硅；铸造；晶粒细化；热处理；磨损

(Edited by Sai-qian YUAN)